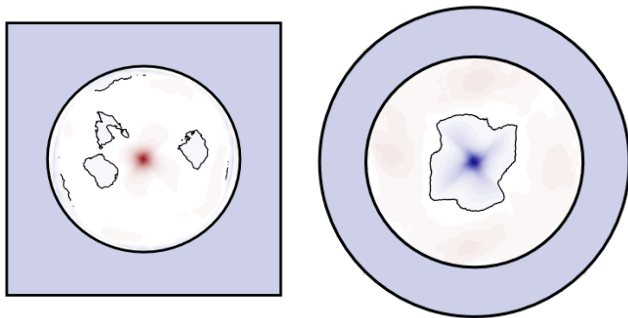
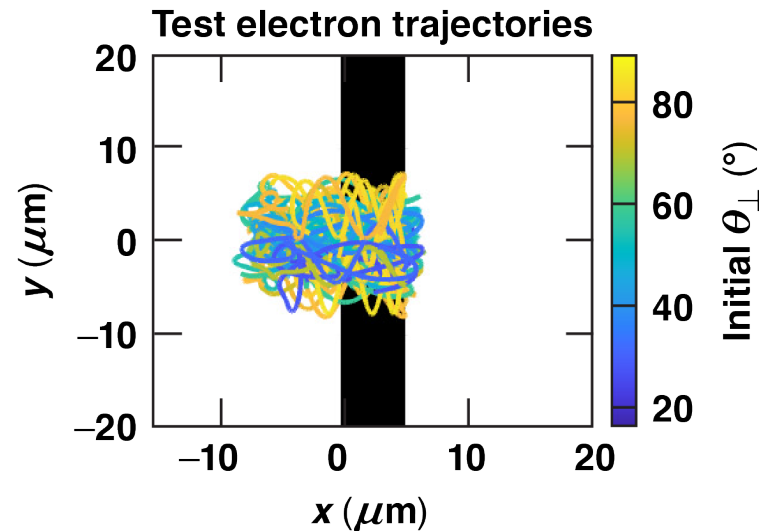


Effects of Kilotesla-Level Magnetic Fields on Relativistic Laser–Plasma Interaction

Magnetic-field generation

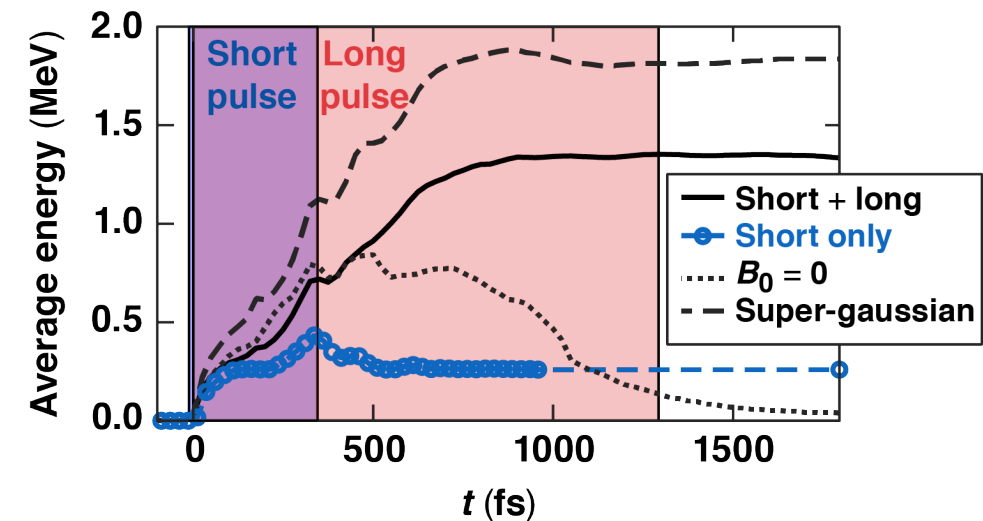


Plasma expansion and sheaths



TC15821a

Direct laser acceleration and plasma heating



TC15827a

K. Weichman
Pronouns: they/them
University of Rochester
Laboratory for Laser Energetics

63rd Annual Meeting of the APS Division of Plasma Physics
8 – 12 November 2021

Kilotesla-level applied magnetic fields introduce new possibilities for relativistic laser–plasma interaction

- Currently available magnetic fields appear “weak” by bulk metrics, yet are sufficiently strong to influence laser-plasma dynamics
- Laser plasmas with embedded magnetic fields do not always behave diamagnetically
- Applied magnetic fields can dramatically change plasma expansion
- Kilotesla or subkilotesla fields can enable new forms of direct laser acceleration-based heating
- Applied magnetic fields open the door to many additional phenomena

Near-term experimentally relevant magnetic fields enable new, useful phenomena in relativistic laser–plasma interactions.

Collaborators



A. V. Arefiev, H. Mao, and F. N. Beg



J. P. Palastro



A. P. L. Robinson



M. Murakami and S. Fujioka



J. J. Santos



T. Tuncian



T. Ditmire and H. Quevedo



Y. Shi



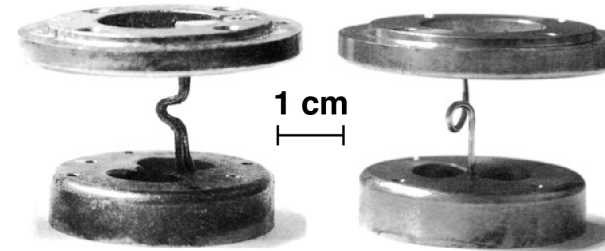
V. V. Ivanov



How strong are experimentally available magnetic fields?

- “Obvious” effects require strong magnetic fields

- $B_0 > B_{\text{laser}}$
- cyclotron resonance ($\omega_{ce} \gtrsim \omega_{\text{laser}}$)
- direct magnetization ($\beta_e = \frac{8\pi n_e T_e}{B_0^2} < 1$)

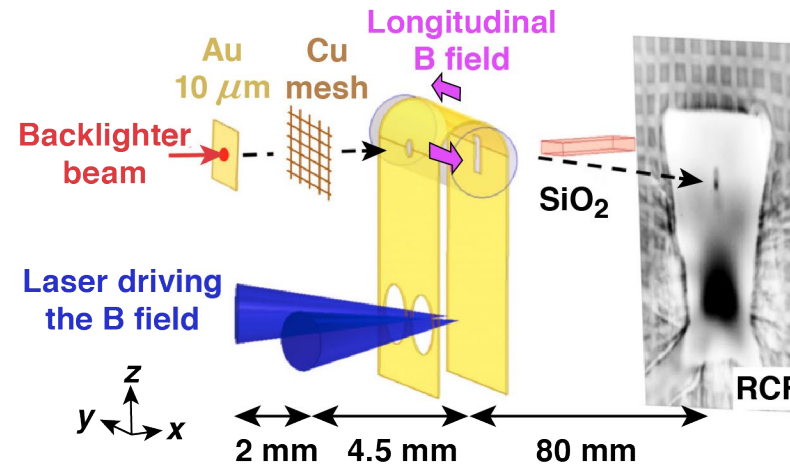


TC15813a

V. V. Ivanov *et al.*, Rev. Sci. Instrum. **89**, 033504 (2018).

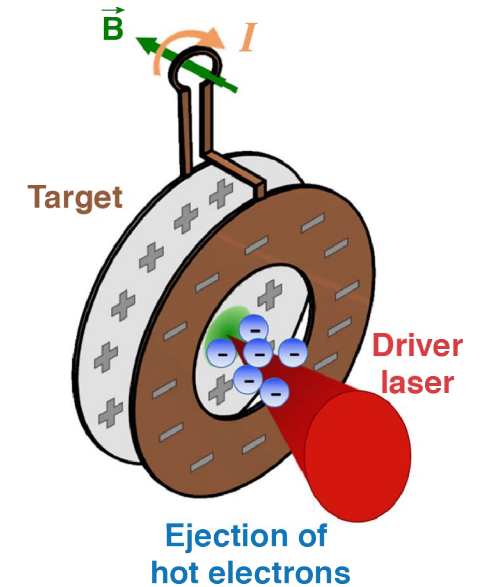


G. Fiksel *et al.*, Rev. Sci. Instrum. **86**, 016105 (2015).



TC15813

C. Goyon *et al.*, Phys. Rev. E **95**, 033208 (2017).



J. J. Santos *et al.*, Phys. Plasmas **25**, 056705 (2018).

RCF: radiochromic film

How strong are experimentally available magnetic fields?

- “Obvious” effects require strong magnetic fields

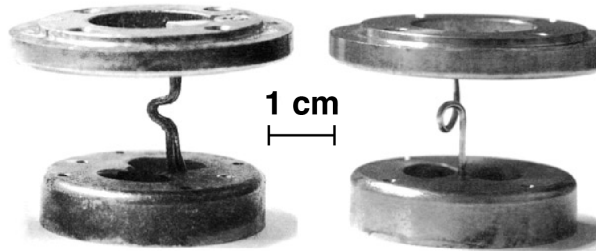
- $B_0 > B_{\text{laser}}$
- cyclotron resonance ($\omega_{\text{ce}} \gtrsim \omega_{\text{laser}}$)
- direct magnetization ($\beta_e = \frac{8\pi n_e T_e}{B_0^2} < 1$)

- State-of-the art magnetic fields reach 100 T to 1 kT

- Compare to fs- to ps-duration pulses with $a_0 = \frac{|e|E_{\text{laser}}}{m_e c \omega_{\text{laser}}} \sim 1 - 3$:

- $B_0/B_{\text{laser}} \lesssim 1/10$
- $\omega_{\text{ce}}/\omega_{\text{laser}} \lesssim 1/10$
- $\beta_e \gtrsim 20$

A kilotesla magnetic field is “weak” by bulk metrics, yet can still have a strong impact.

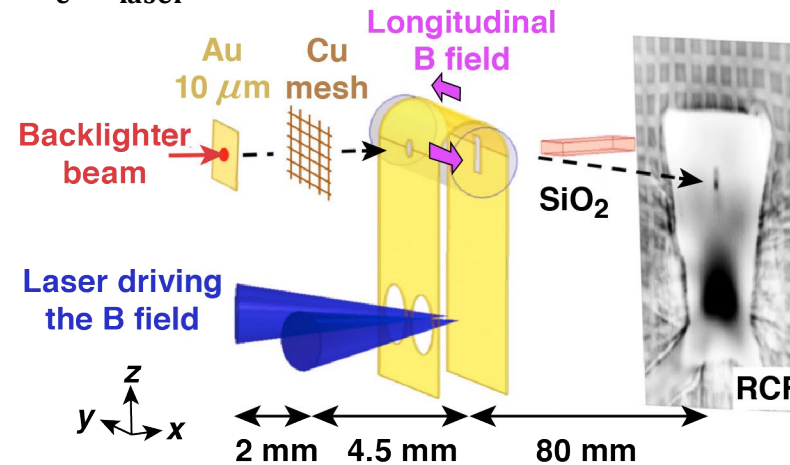


TC15813a

V. V. Ivanov et al., Rev. Sci. Instrum. **89**, 033504 (2018).

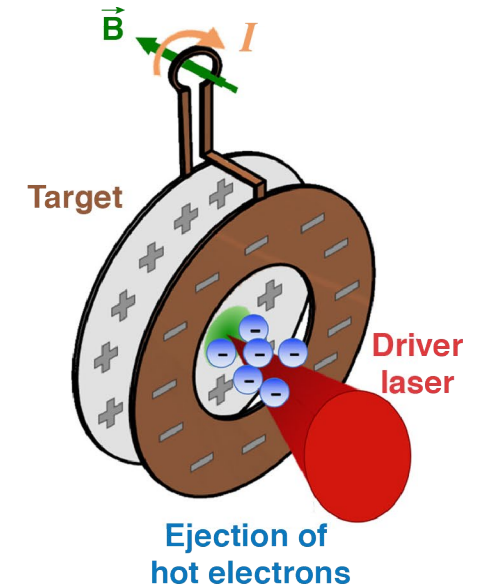


G. Fiksel et al., Rev. Sci. Instrum. **86**, 016105 (2015).



TC15813

C. Goyon et al., Phys. Rev. E **95**, 033208 (2017).

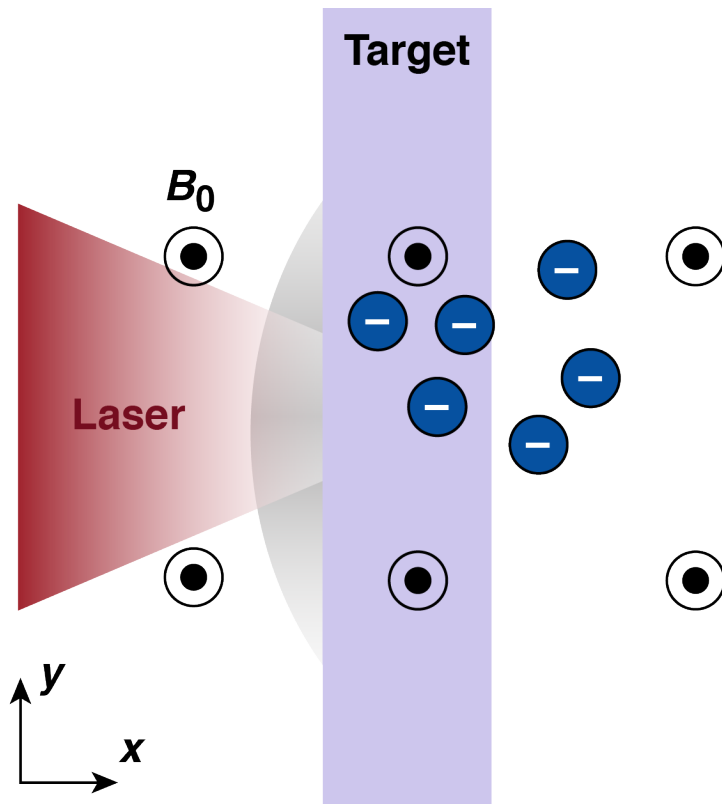


J. J. Santos et al., Phys. Plasmas **25**, 056705 (2018).

RCF: radiochromic film

A relativistic laser produced plasma is not always diamagnetic and can generate magnetic fields

$B_{z0} = 100 \text{ T to } 1 \text{ kT}$



TC15814a

Opaque target

2- μm thick CH $< \rho_L$
0.1- μm preplasma
scale length

Laser

$1 \times 10^{19} \text{ W/cm}^2$
100 fs FWHM
 $\lambda = 0.8 \mu\text{m}$
y polarized

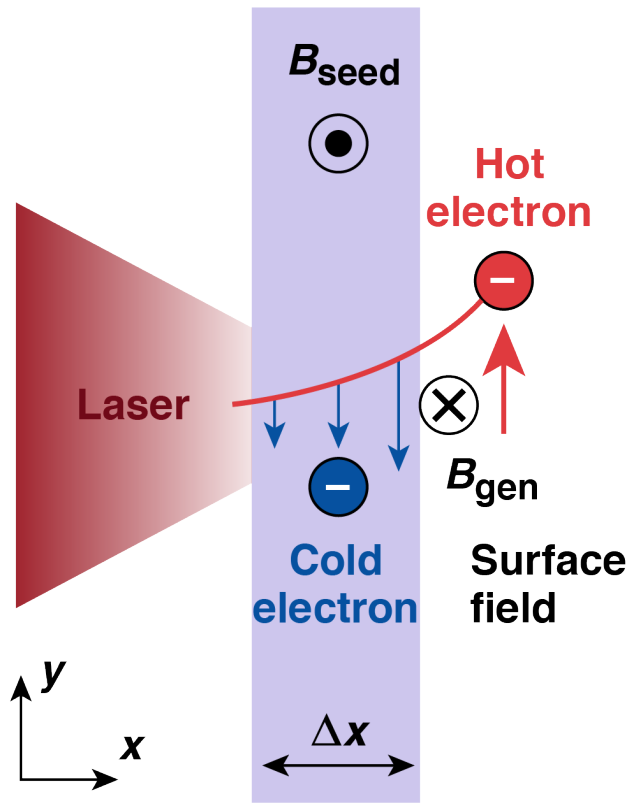
Simulations

1-D and 2-D
EPOCH PIC code

- (Hypothetical) diamagnetic picture
 - laser generates hot plasma
 - current in hot plasma reduces the applied magnetic field

K. Weichman *et al.*, New J. Phys. **22**, 113009 (2020).
PIC: particle in cell

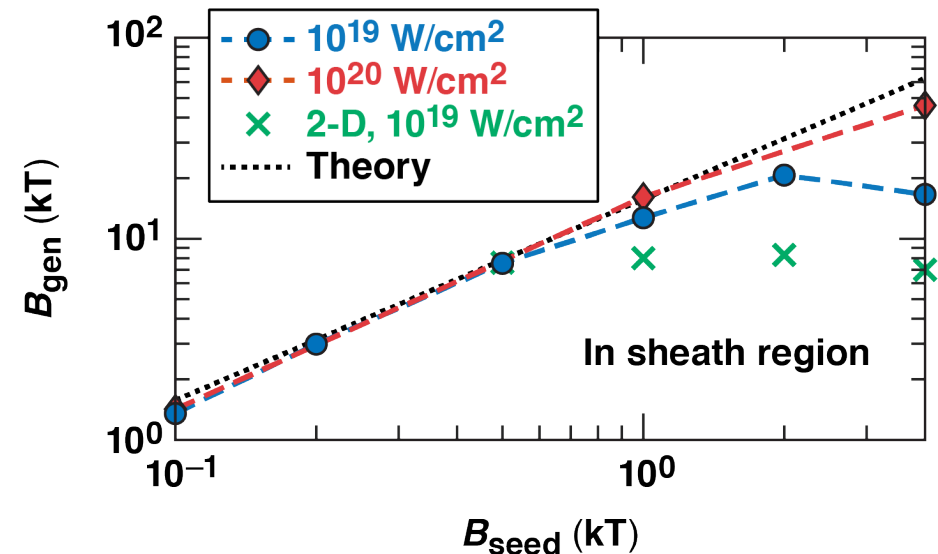
Surface field generation is an overshoot of the diamagnetic effect



TC15814

Surface magnetic field generation is a kinetic effect.

- Cyclotron rotation of hot electrons originating at the laser-plasma interface leads to a net transverse current
- Hot electron current is screened by cold population within the target, allowing it to overshoot the usual diamagnetic limit
- The magnetic-field estimate based on cyclotron rotation agrees well with observed fields (for $\Delta x < \rho_L$)



TC15815

K. Weichman et al., New J. Phys. **22**, 113009 (2020).

Surface magnetic-field generation can have surprising consequences

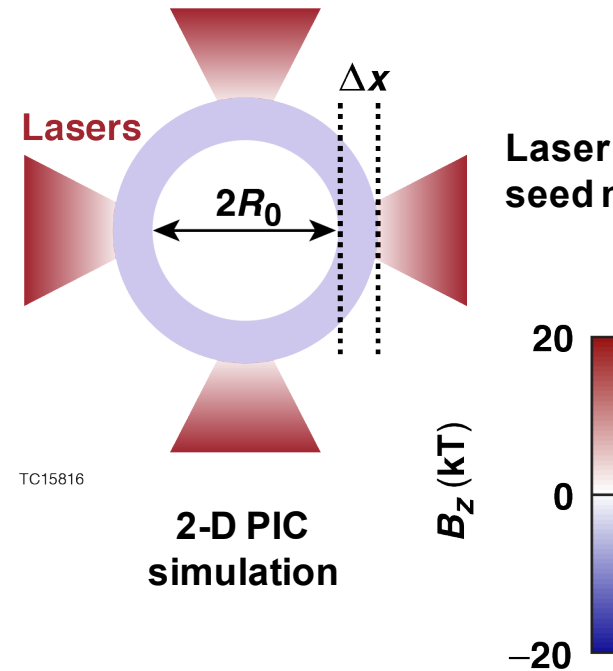
- Microtube implosions generate and amplify magnetic fields

- Microtube target

- 3- μm thick CH shell
- 3- μm radius central void
- four lasers

- Lasers

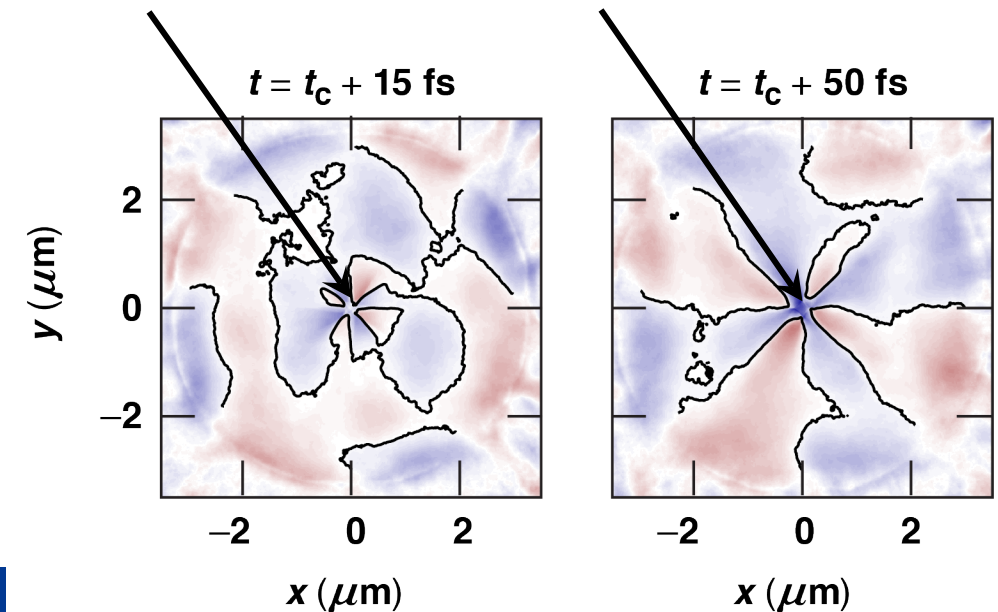
- $1 \times 10^{21} \text{ W/cm}^2$
- 15 μm FWHM
- 25 fs FWHM
- $\lambda = 0.8 \mu\text{m}$
- y polarized



Initially unmagnetized ($B_{z0} = 0$) case

Laser asymmetry provides seed magnetic field

B is amplified by electron current after ions reach center ($E \times B$)



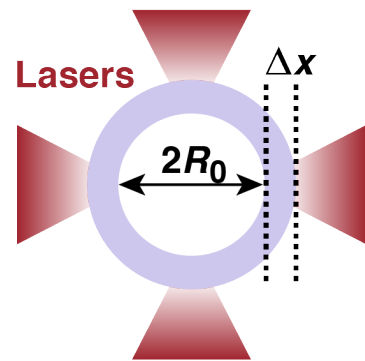
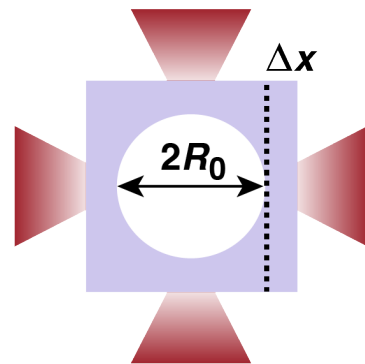
Any magnetic field present can be amplified by the implosion.

M. Murakami *et al.*, Sci. Rep. **10**, 16653 (2020).
K. Weichman *et al.*, Appl. Phys. Lett. **117**, 244101 (2020).

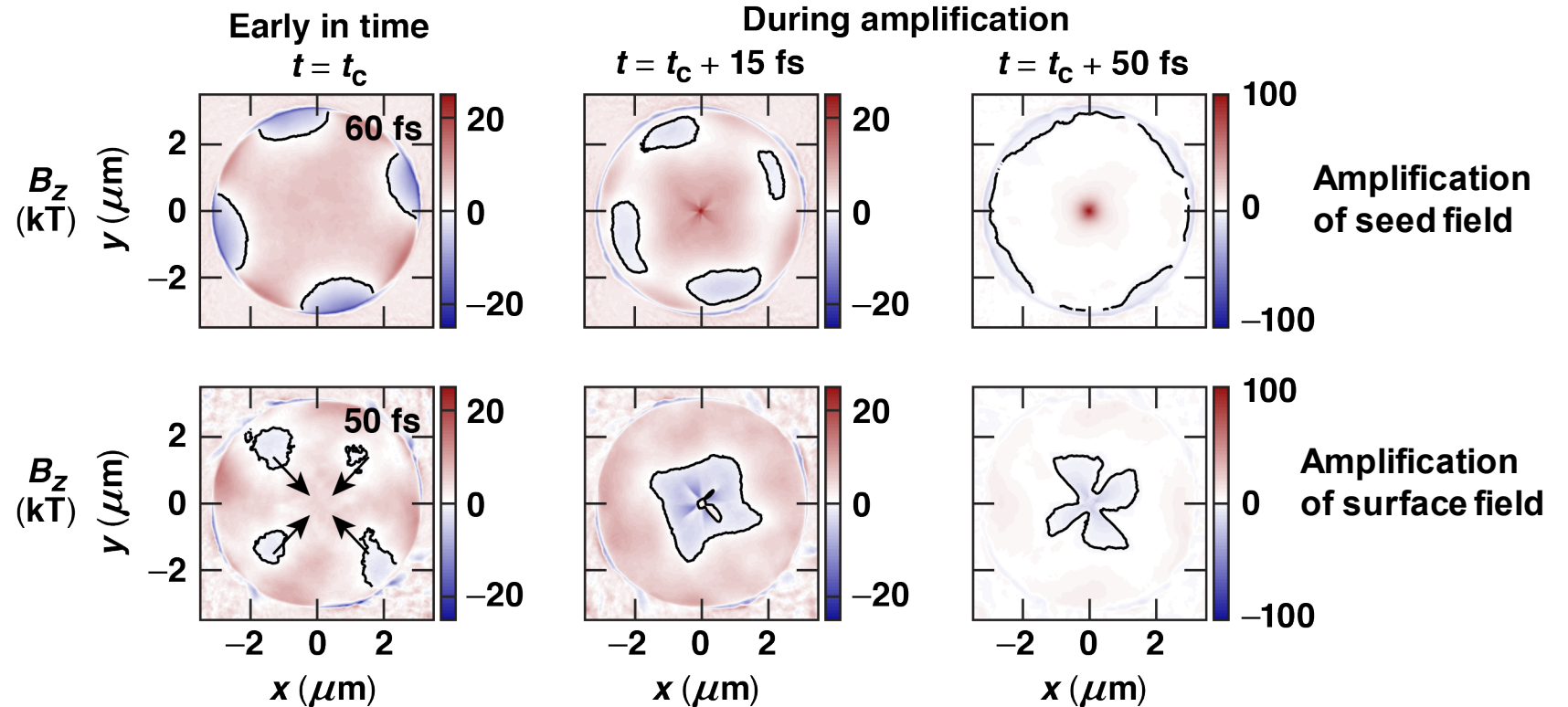
The sign of the amplified field can be reversed due to surface magnetic-field generation

Seed magnetic fields enable strong magnetic-field generation

⊙ $B_{z0} = 3 \text{ kT}$



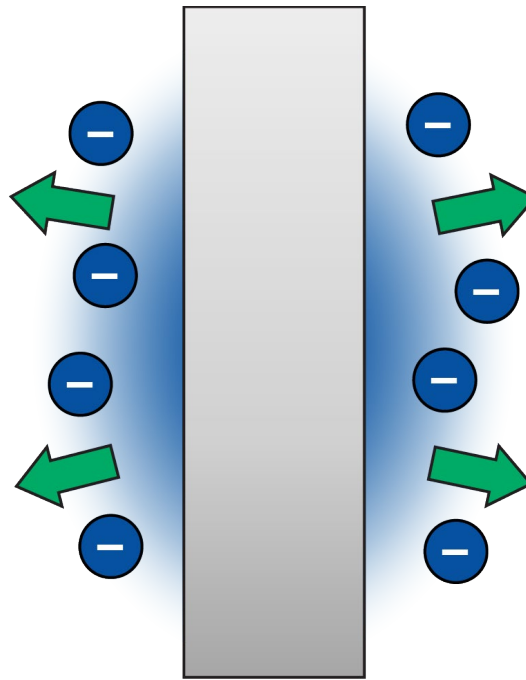
TC15816a



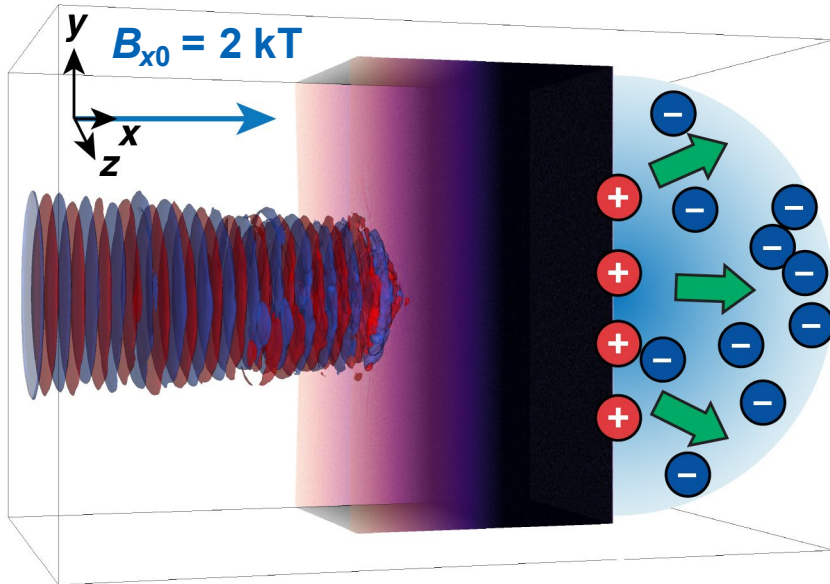
TC15818

K. Weichman *et al.*, Appl. Phys. Lett. **117**, 244101 (2020).

Plasma expansion and sheaths



Target-normal applied magnetic fields can enhance sheath-based ion acceleration



TC15819

Opaque target

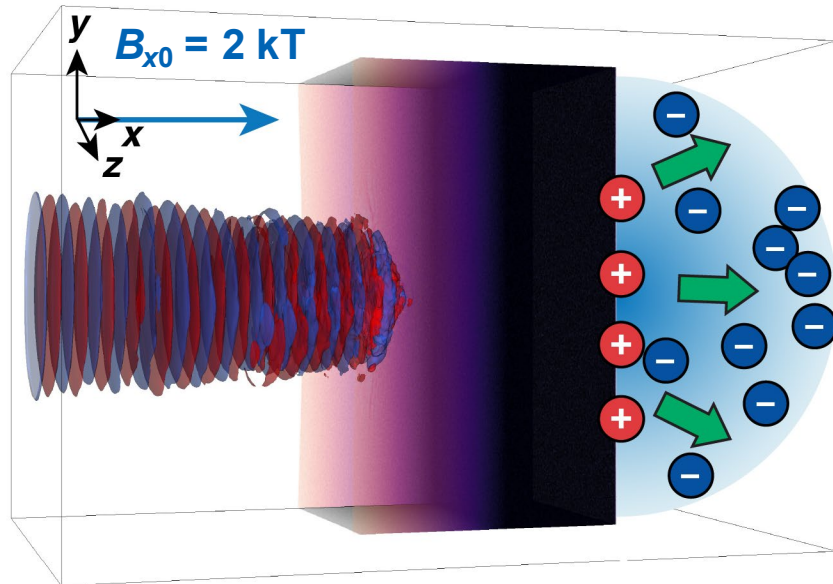
5- μm thick CH
1.5- μm -preplasma
scale length

3-D simulation

Laser

$2 \times 10^{19} \text{ W/cm}^2$
3 μm FWHM
150 fs FWHM
 $\lambda = 1 \mu\text{m}$
y polarized

Target-normal applied magnetic fields can enhance sheath-based ion acceleration



TC15819

Opaque target

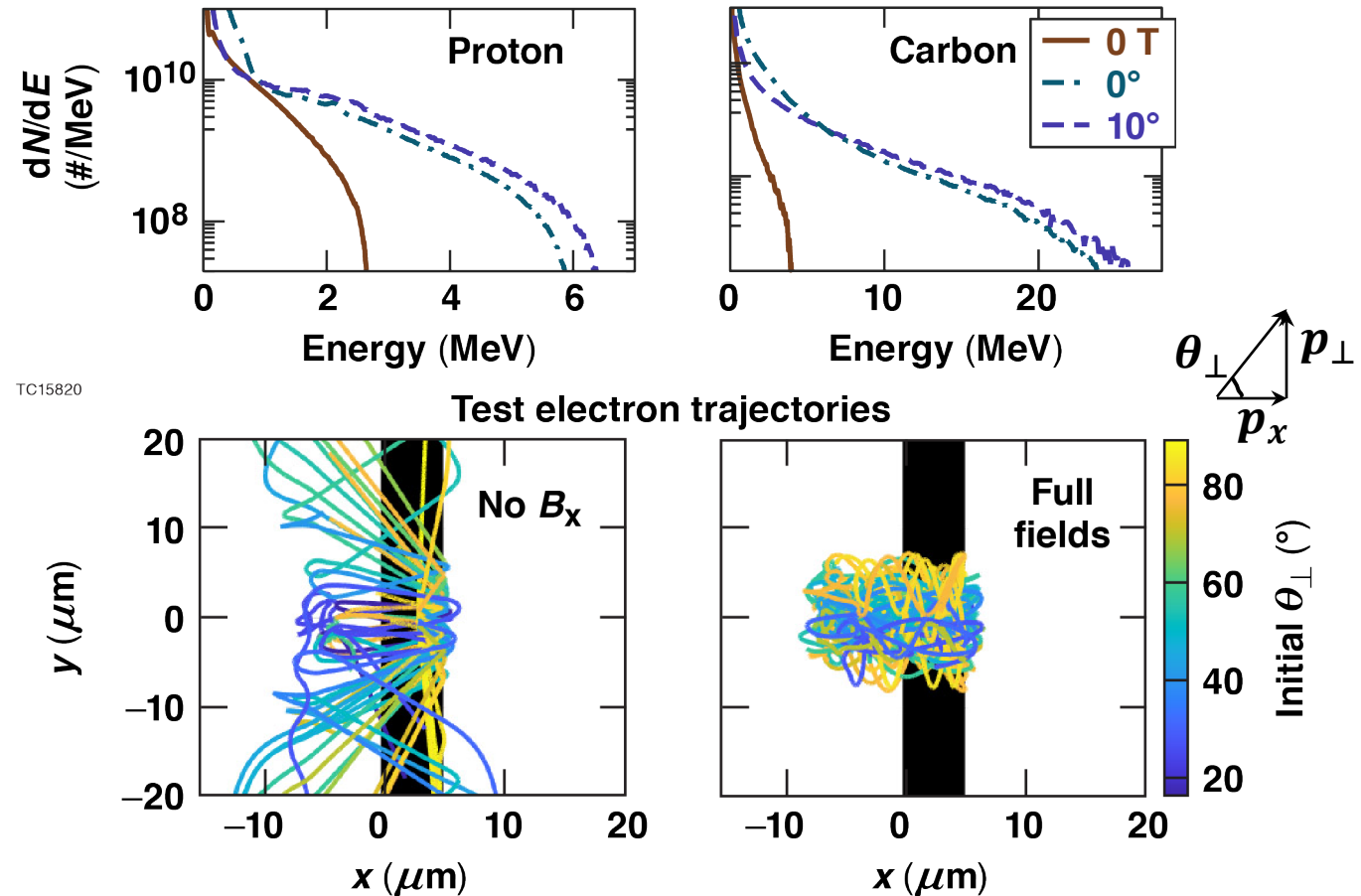
5- μm thick CH
1.5- μm -preplasma
scale length

3-D simulation

Laser

$2 \times 10^{19} \text{ W/cm}^2$
3 μm FWHM
150 fs FWHM
 $\lambda = 1 \mu\text{m}$
y polarized

Target thickness \sim Larmor radius
substantially increases ion energy and number

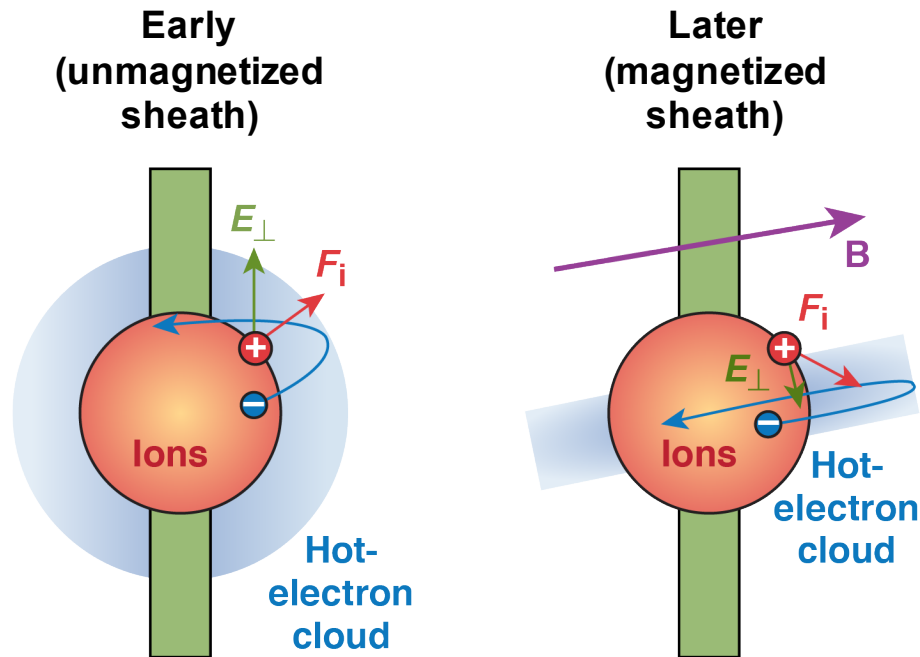


K. Weichman *et al.*, Sci. Rep. **10**, 18966 (2020).

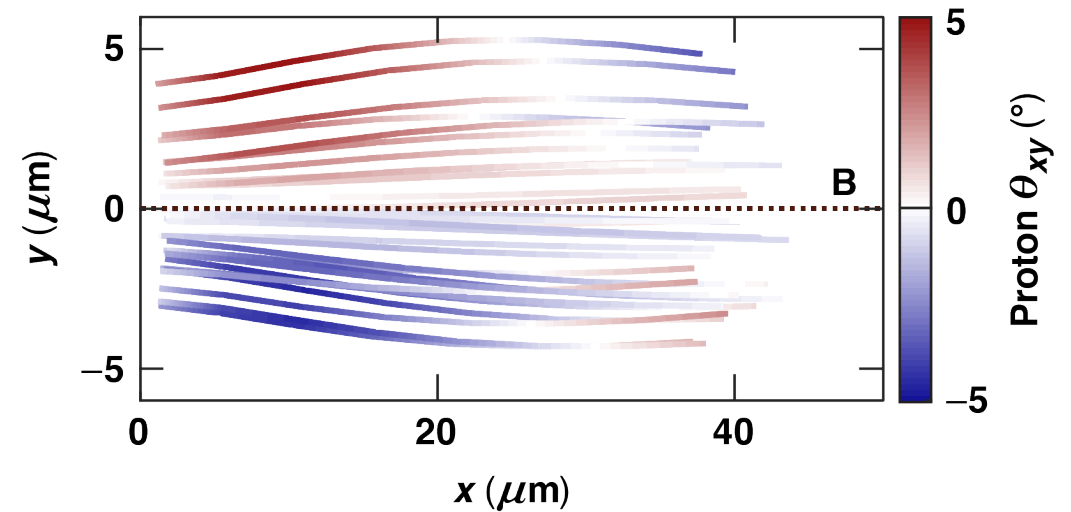
(Eventual) magnetization of sheath induces ion focusing

$$\text{Magnetization: } \frac{E_{\text{sheath}}}{B_0} \sim \sqrt{\frac{4\pi n_e T_e}{B_0^2}} \sim \sqrt{\beta_e} \lesssim 1$$

- Initially $\beta_e > 1$, but n_e (and β_e) drop during plasma expansion
- Change in E_{\perp} leads to ion focusing



TC15822

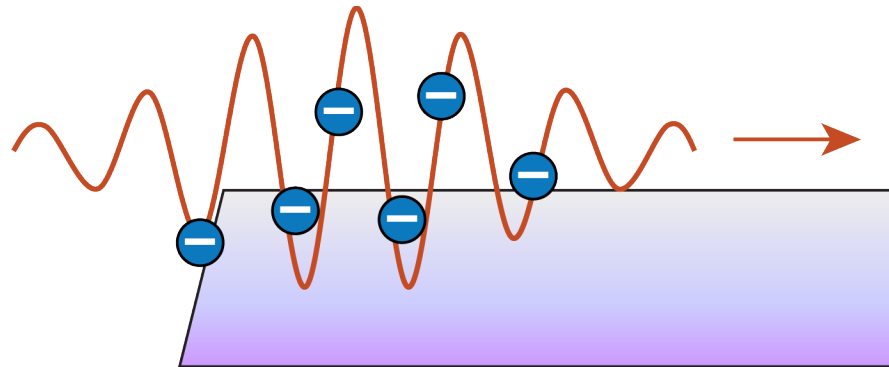


TC15823

A target-normal magnetic field produces a focusing ion source with enhanced energy and numbers.

K. Weichman *et al.*, Sci. Rep. **10**, 18966 (2020).

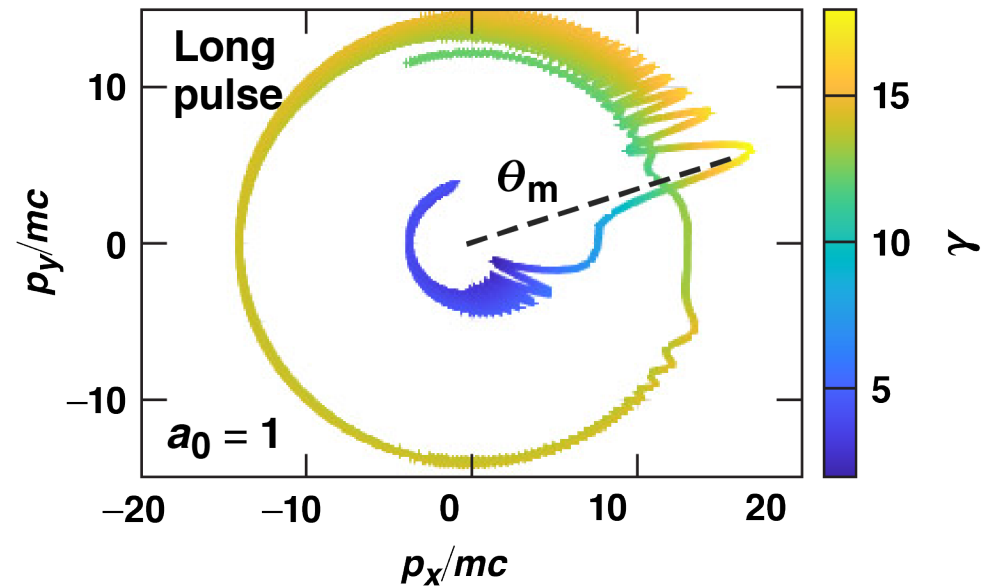
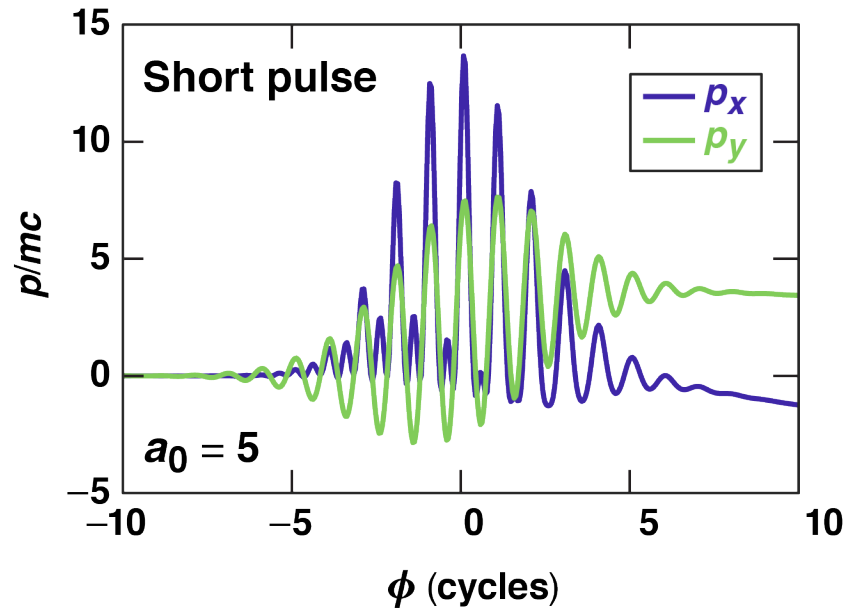
Direct laser acceleration and plasma heating



Applied magnetic fields enable new regimes in direct laser acceleration

A transverse magnetic field (B_{z0} with y -polarized laser) enables electron energy retention

- Partial cyclotron rotation
 - initially cold plasma
 - pulse duration < cyclotron period
 - $\gamma_{\text{final}} \lesssim a_0$
- Magnetically assisted kicks
 - initially hot plasma
 - pulse duration \gg cyclotron period
 - $\gamma_{\text{final}} \sim a_0^{3/2} (\omega_{\text{laser}}/\omega_{\text{ce}})^{1/2}$



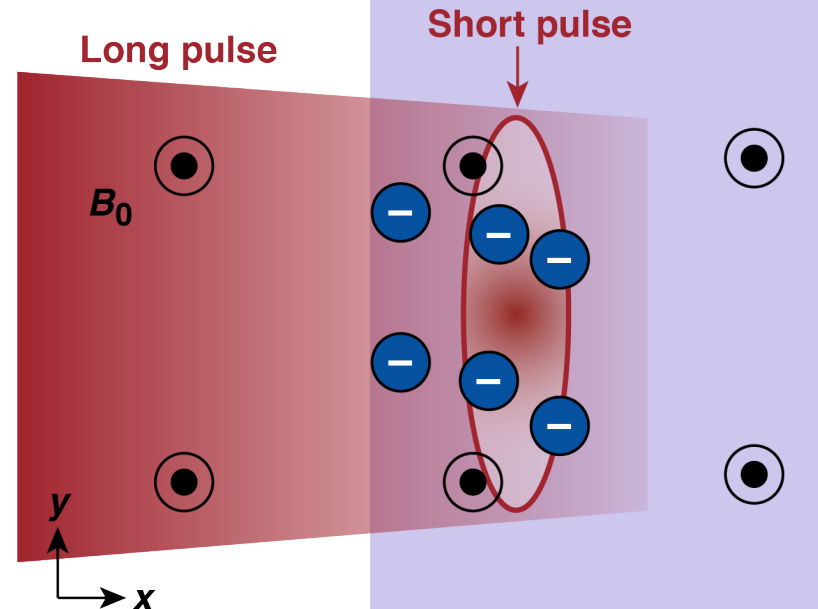
TC15824

These acceleration strategies can be combined.

A. P. L. Robinson and A. V. Arefiev, Phys. Plasmas **27**, 023110 (2020).
A. Arefiev, Z. Gong, and A. P. L. Robinson, Phys. Rev. E **101**, 043201 (2020).

Magnetized direct laser acceleration can create a relativistic, underdense thermal plasma

$B_{z0} = 100$ to 500 T



TC15829

**Femtosecond
laser**

$a_0 = 5$
20 fs FWHM

Plasma

**Picosecond
laser**

$a_0 = 1$
0.8 ps FWHM

10^{-3} to $10^{-2} n_c$
100- μ m-thick-H

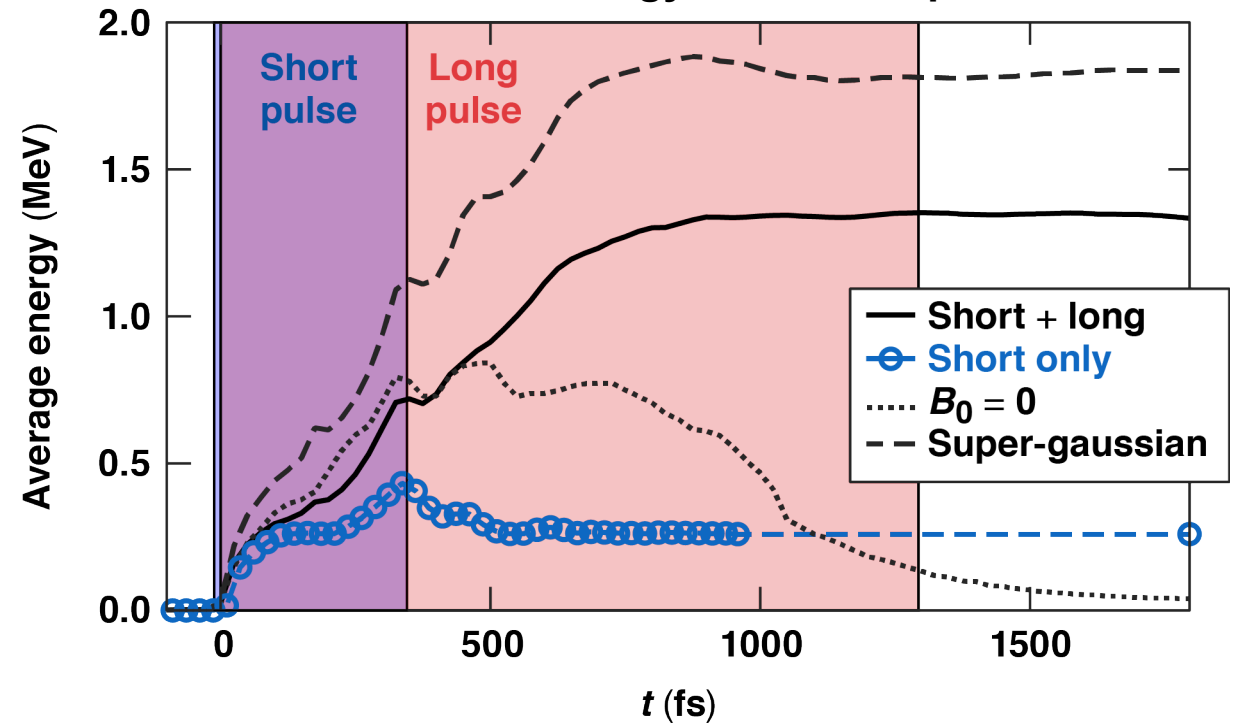
Both lasers

100 μ m FWHM
 $\lambda = 1 \mu$ m

2-D simulation

TC15827

Relativistic energy retained in plasma

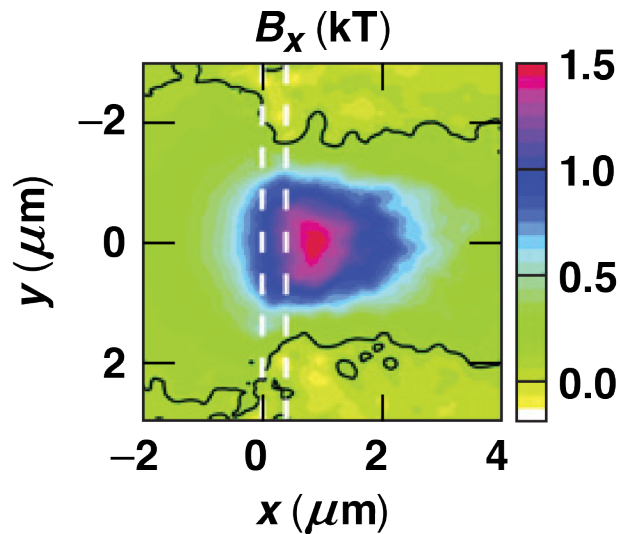


**Magnetic fields enable relativistic plasma generation
in an otherwise difficult-to-access regime.**

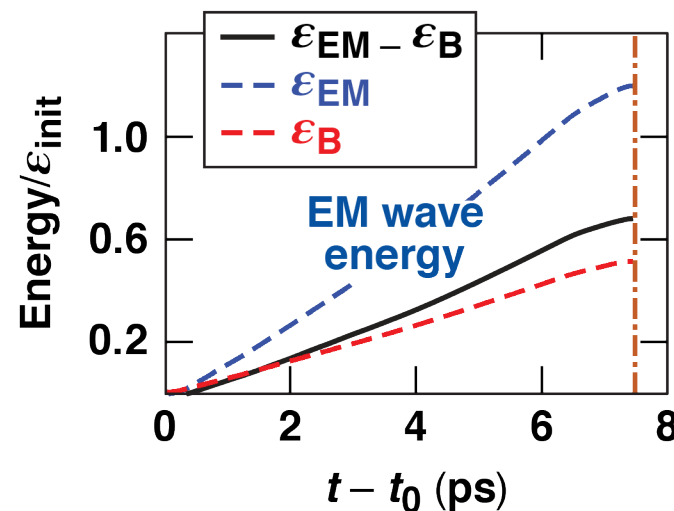
Magnetized relativistic laser-plasma physics offers many additional phenomena

A few examples

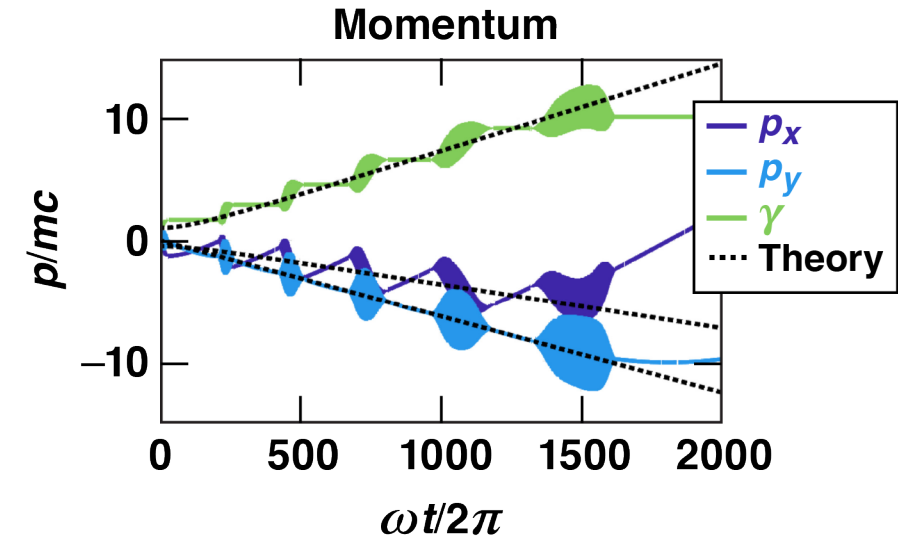
Magnetic-field
amplification in a solid by
return current*



Electromagnetic wave
generation during plasma
expansion into neutral gas**



Multiple cycles of
ponderomotive energy gain
(e.g., by a flying focus pulse)



TC15828

* Y. Shi et al., New J. Phys. **22**, 073067 (2020).
H. Mao et al., Phys. Rev. E **103, 023209 (2021).

Kilotesla-level applied magnetic fields introduce new possibilities for relativistic laser–plasma interaction

- **Currently available magnetic fields appear “weak” by bulk metrics, yet are sufficiently strong to influence laser-plasma dynamics**
- **Laser plasmas with embedded magnetic fields do not always behave diamagnetically**
- **Applied magnetic fields can dramatically change plasma expansion**
- **Kilotesla or subkilotesla fields can enable new forms of direct laser acceleration-based heating**
- **Applied magnetic fields open the door to many additional phenomena**

Near-term experimentally relevant magnetic fields enable new, useful phenomena in relativistic laser–plasma interactions.

Backup slides

Scale comparison for 1 kT



Typical parameters for modestly relativistic laser-plasma

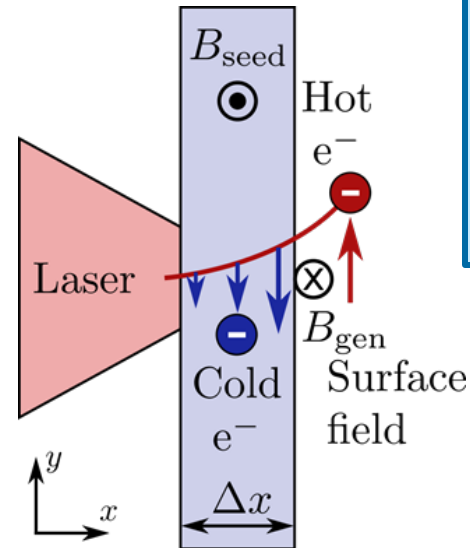
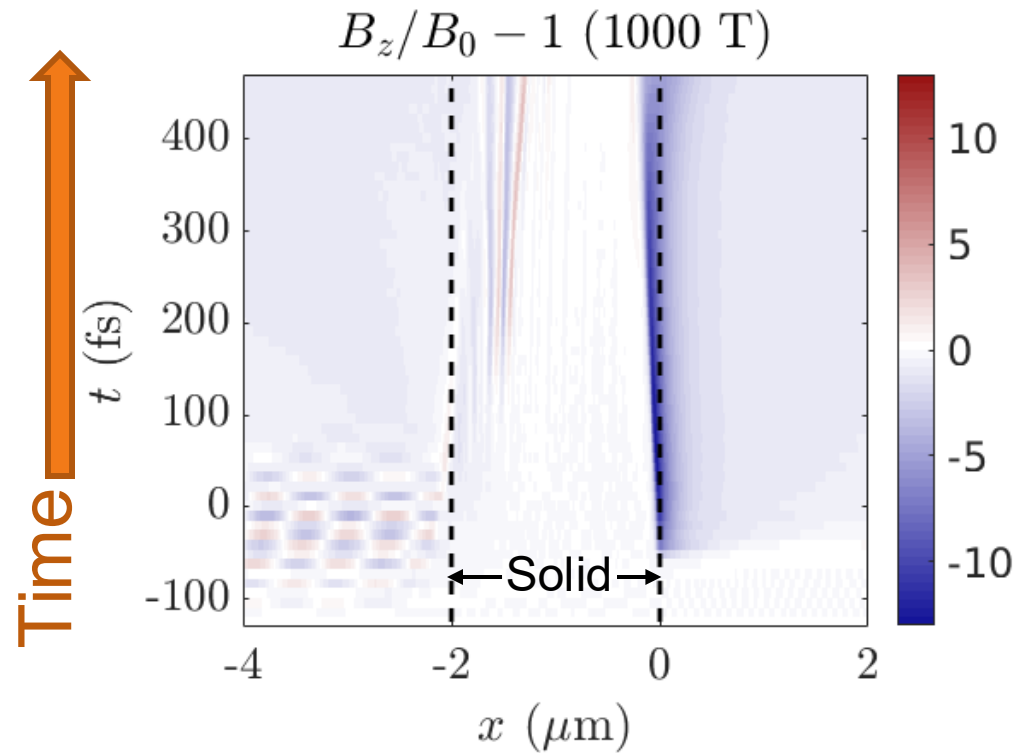
Laser parameters	Value	Plasma parameters	Value
Laser amplitude	$a_0 = e E_0/m_e c \omega \sim 1 - 3$ $(\sim 10^{19} \text{ W/cm}^2)$	Hot electron temperature	$T_e \sim \text{MeV}$
Pulse duration	100 fs – 10 ps	Plasma density (hot part)	$n_e \sim 10^{-4} - 1 n_{cr}$ $\sim 10^{17} - 10^{21} \text{ cm}^{-3}$

Laser-plasma scales	Magnetic field scales	Comparison
Laser frequency	Cyclotron frequency	$\omega_{laser}/\omega_{ce} \gtrsim 10$
Laser field B_{laser}	Applied field B_0	$B_{laser}/B_0 \gtrsim 10$
Thermal pressure	Magnetic field pressure	$\beta_e = 8\pi n_e T_e/B_0^2 \sim 20 - 500$
Scale of electron motion l	Larmor radius ρ_L	$\rho_L/l \sim 1 - 10$

Surface magnetic field generation

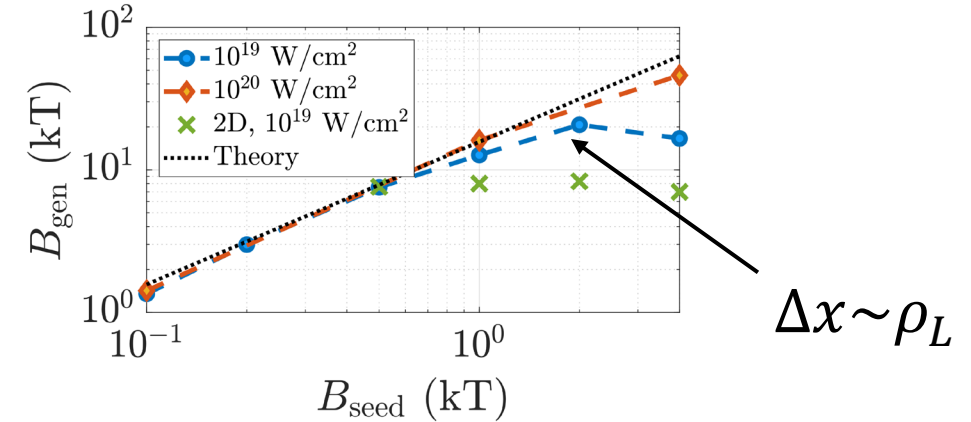
$B_{z0} = 1 \text{ kT}$ generates $> 10 \text{ kT}$

Strong magnetic field generation is due to cyclotron rotation of hot electrons in target



Estimate based on momentum rotation in target ($\Delta x < \rho_L$)

$$\frac{B_{\text{gen}}}{B_{\text{seed}}} \sim -2\pi \frac{\Delta x}{\lambda_{\text{laser}}}$$

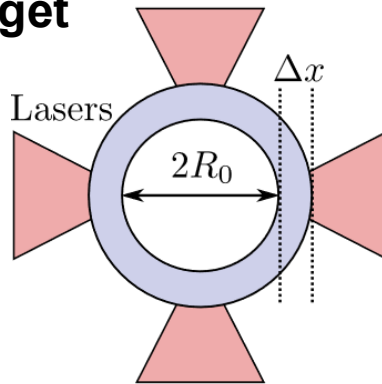


Surface magnetic field generation can have surprising consequences

Microtube implosions generate and amplify magnetic fields

Microtube target

3 μm thick
CH shell
3 μm radius
central void
4 lasers



Lasers

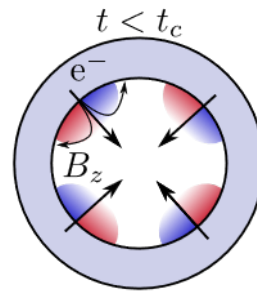
1×10^{21} W/cm²
15 μm FWHM
25 fs FWHM
 $\lambda = 0.8 \mu\text{m}$
y-polarized

2D PIC
simulation

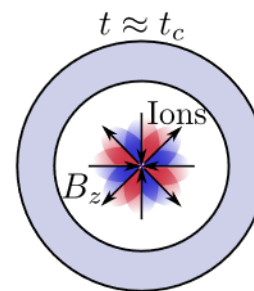
Initially unmagnetized ($B_{z0} = 0$) case

Asymmetry provides
seed magnetic field

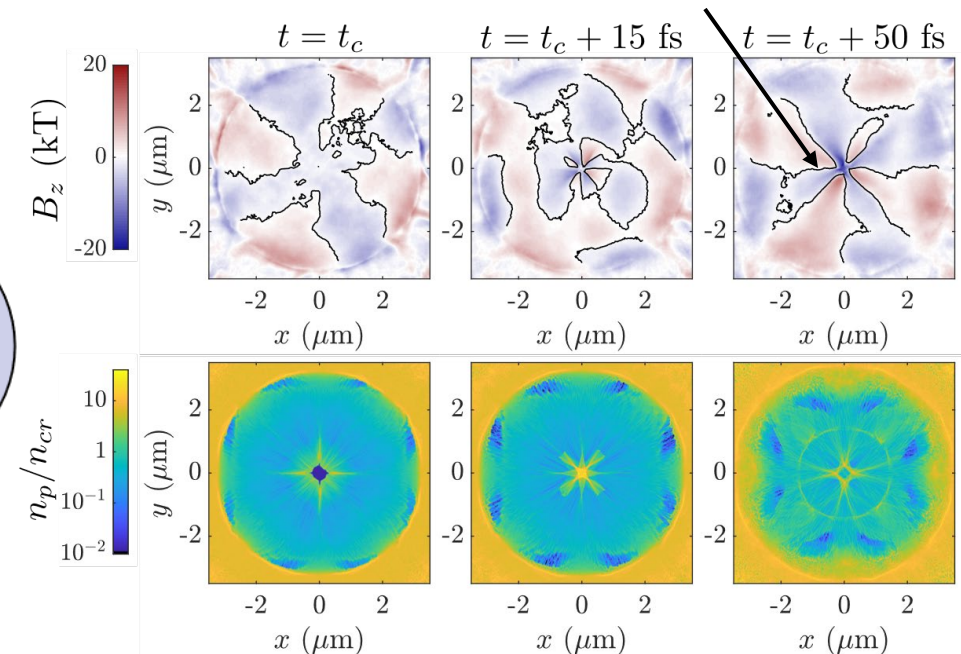
**Early
(electron)**



**Later
(ion)**



B is amplified by electron current
after ions reach center ($E \times B$)

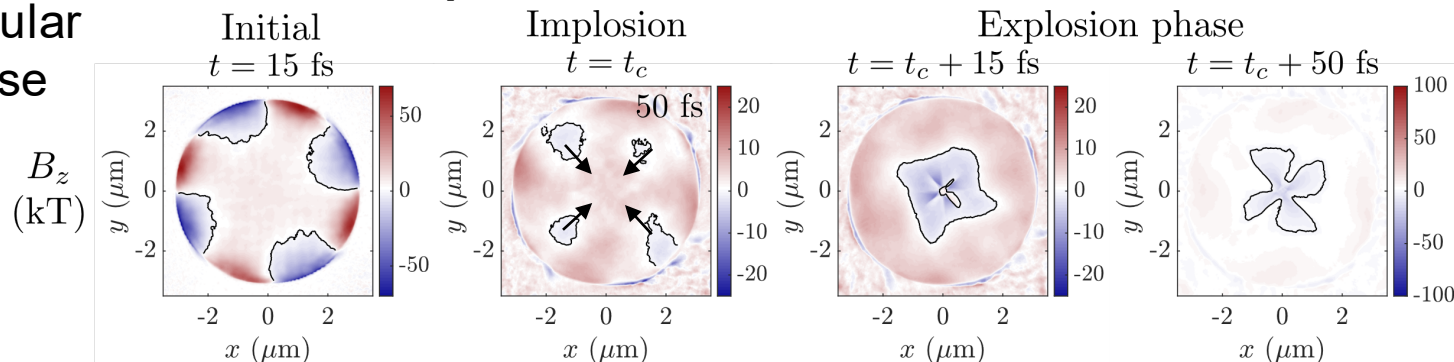


Any magnetic field present can be amplified by the implosion

Polarity of amplified field is sensitive to parameters

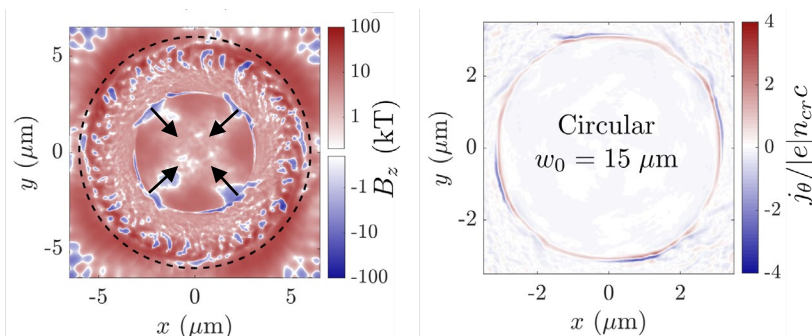
Amplification of surface field

Circular case

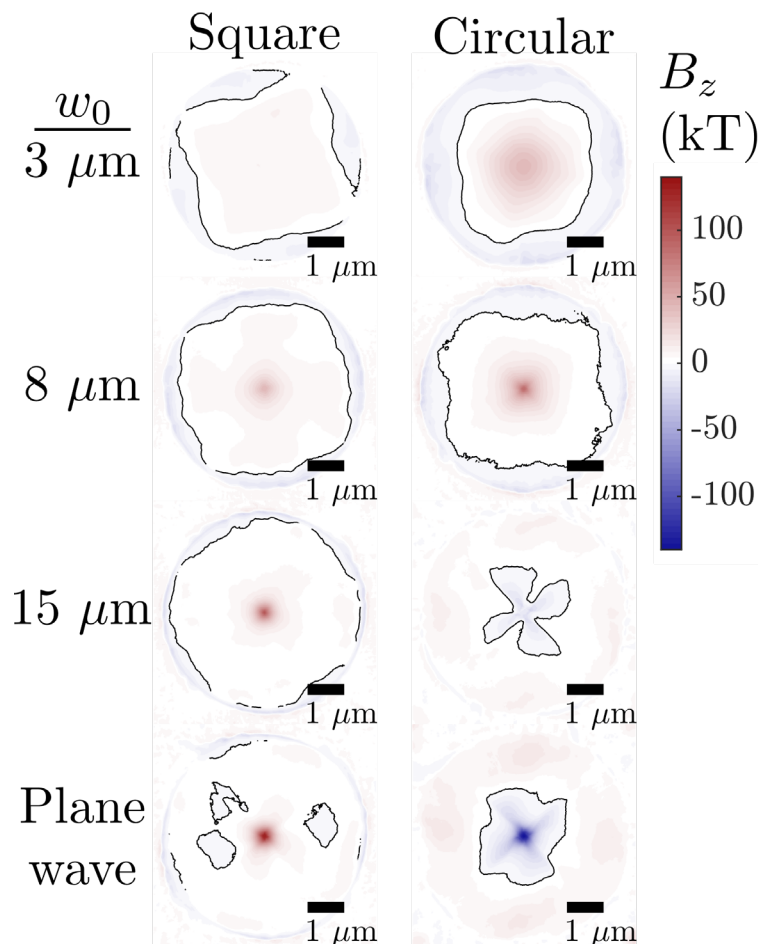
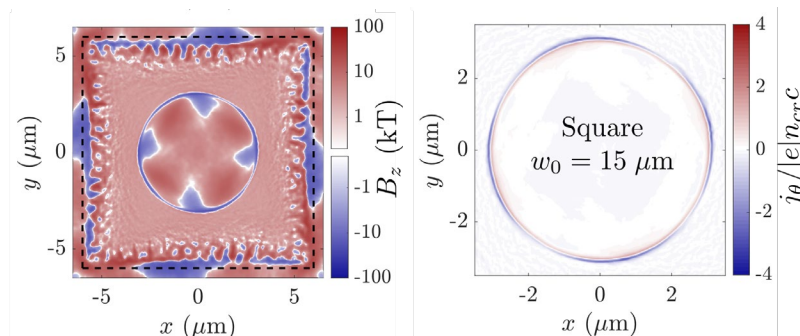


When surface magnetic field is unstable, it can be amplified in lieu of the seed

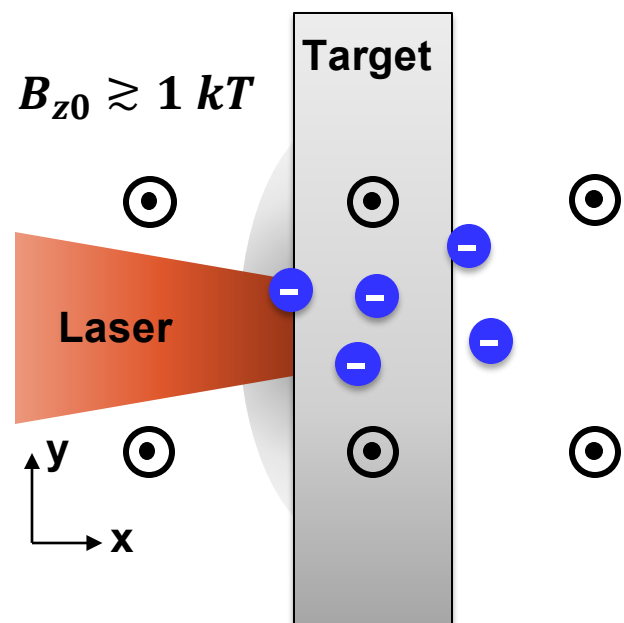
Unstable



Stable



Transverse magnetic fields can also affect target expansion



Opaque target

$2 \mu\text{m}$ thick CH
target $\gtrsim \rho_L$
 $0.1 \mu\text{m}$ preplasma
scale length

2D simulation

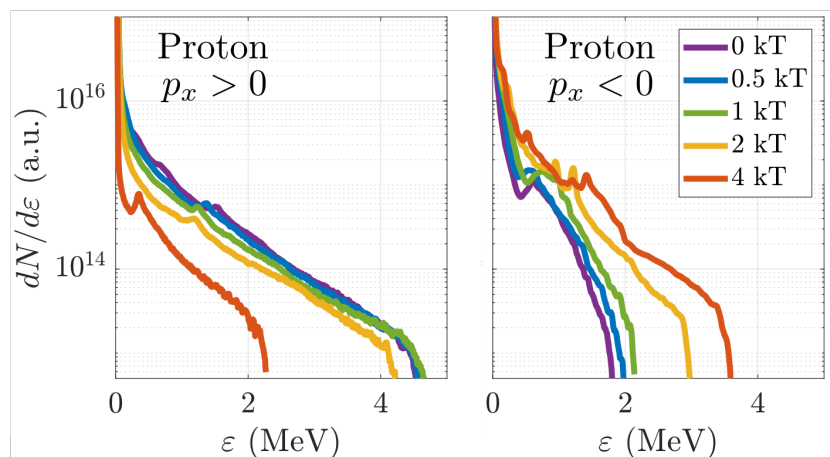
Laser

$1 \times 10^{19} \text{ W/cm}^2$
100 fs FWHM
 $\lambda = 0.8 \mu\text{m}$
y-polarized

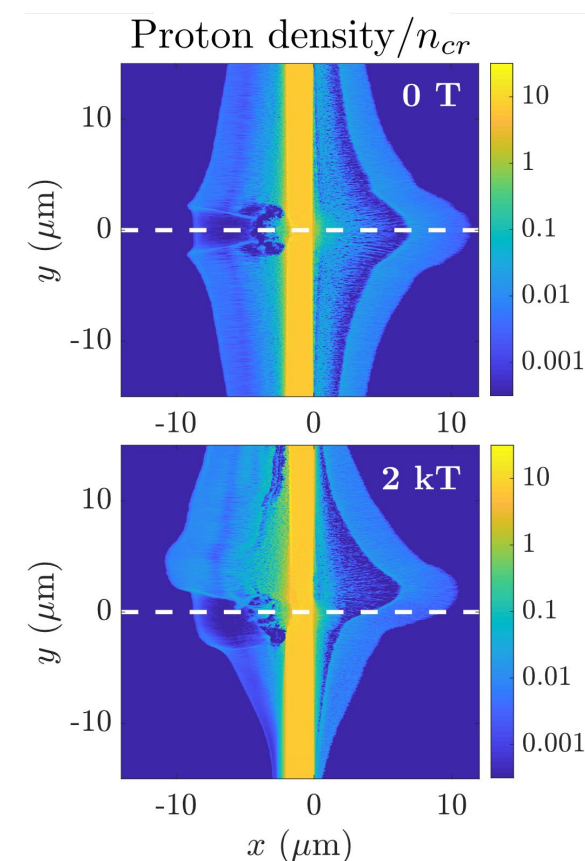
Unusual: acceleration from
the front surface can exceed
the rear surface

Rear surface
(suppressed)

Front surface
(enhanced)

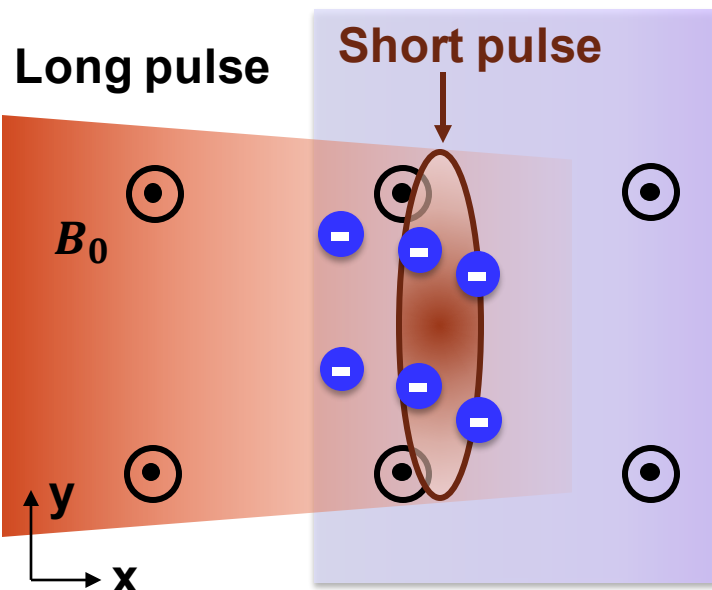


Deflection from
laser axis



Magnetized direct laser acceleration can create relativistic, underdense thermal plasma

$$B_{z0} = 100 - 500 \text{ T}$$



fs laser

$a_0 = 5$
20 fs FWHM

ps laser

$a_0 = 1$
0.8 ps FWHM

Both lasers

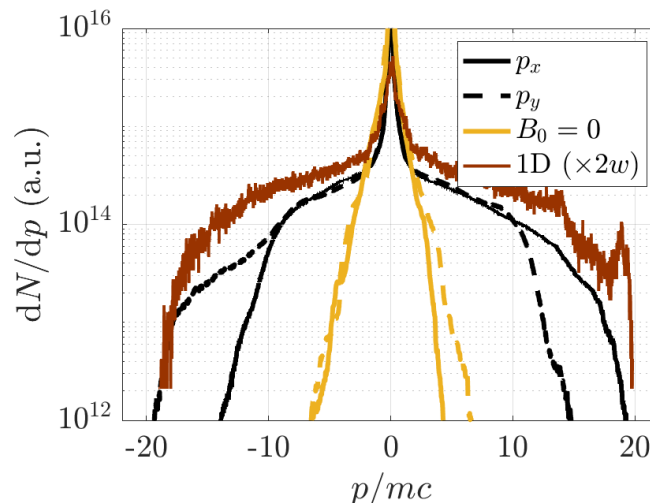
100 μm FWHM
 $\lambda = 1 \mu\text{m}$

Plasma

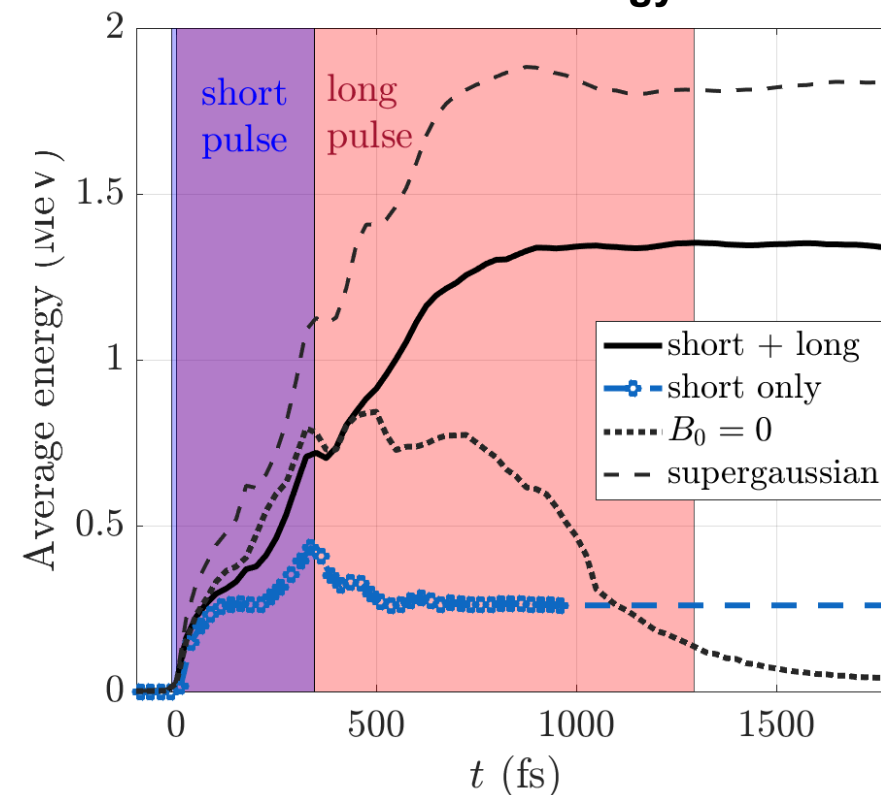
$10^{-3} - 10^{-2} n_{\text{cr}}$
100+ μm thick H

2D simulation

(2D) isotropic spectrum

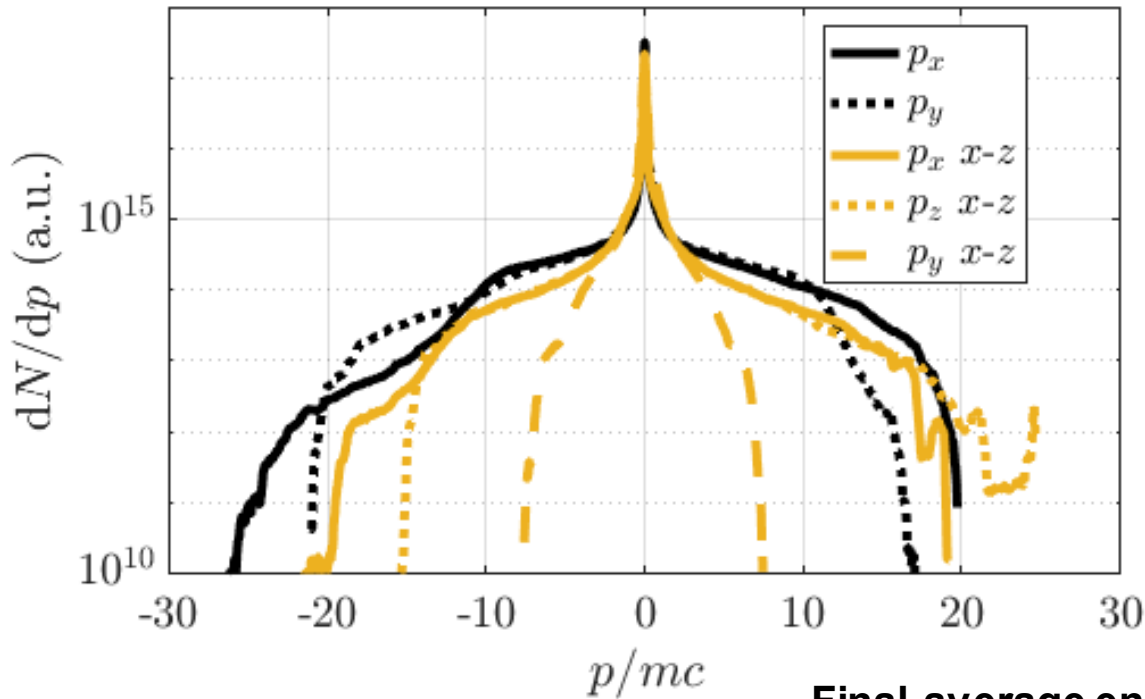


Relativistic energy



Magnetic fields enable relativistic plasma generation in an otherwise difficult-to-access regime

Heating mechanism is robust to electron motion in the third direction



Final average energy: 0.9 MeV

Motion in third direction preserves θ during acceleration, but reduces energy gain

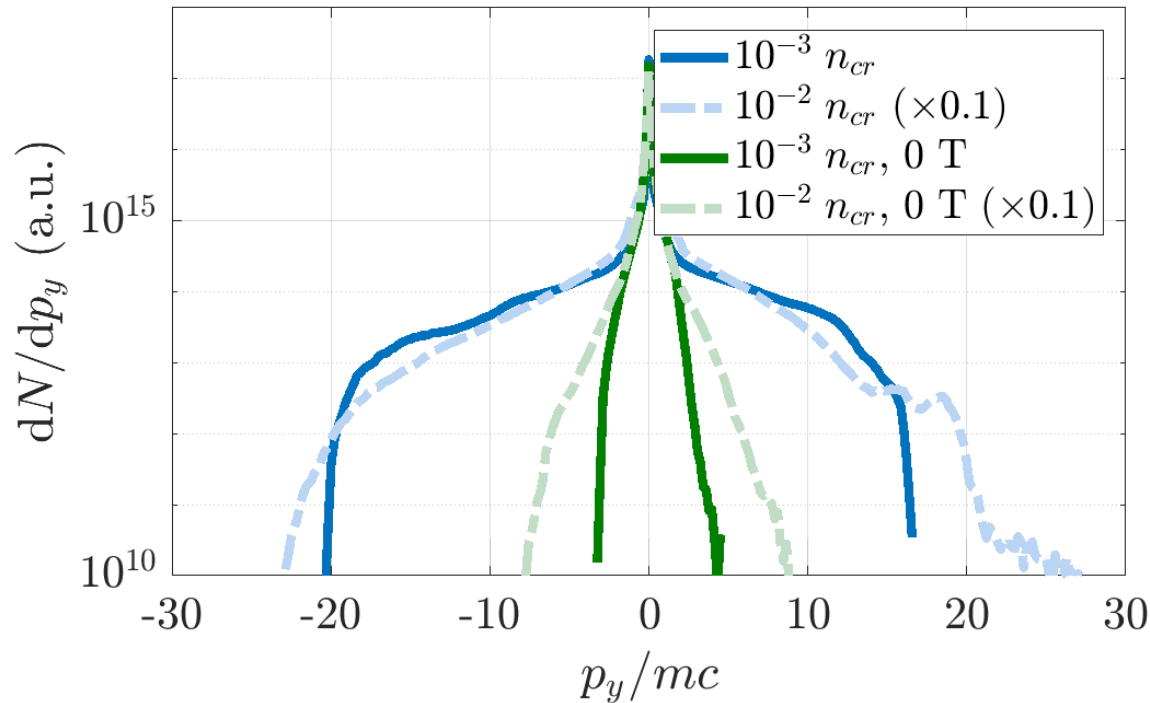
With $p_z \neq 0$

$$p_x = |p| \cos \theta$$

$$\frac{d\theta}{ds} = \sqrt{1 - \frac{p_z^2}{p_y^2 + p_z^2}} \cdot \frac{\frac{\omega_c}{\omega_0} + \left(\frac{1}{\beta} \cos \theta - 1\right) \frac{da}{ds}}{\gamma(1 - \beta \cos \theta)}$$

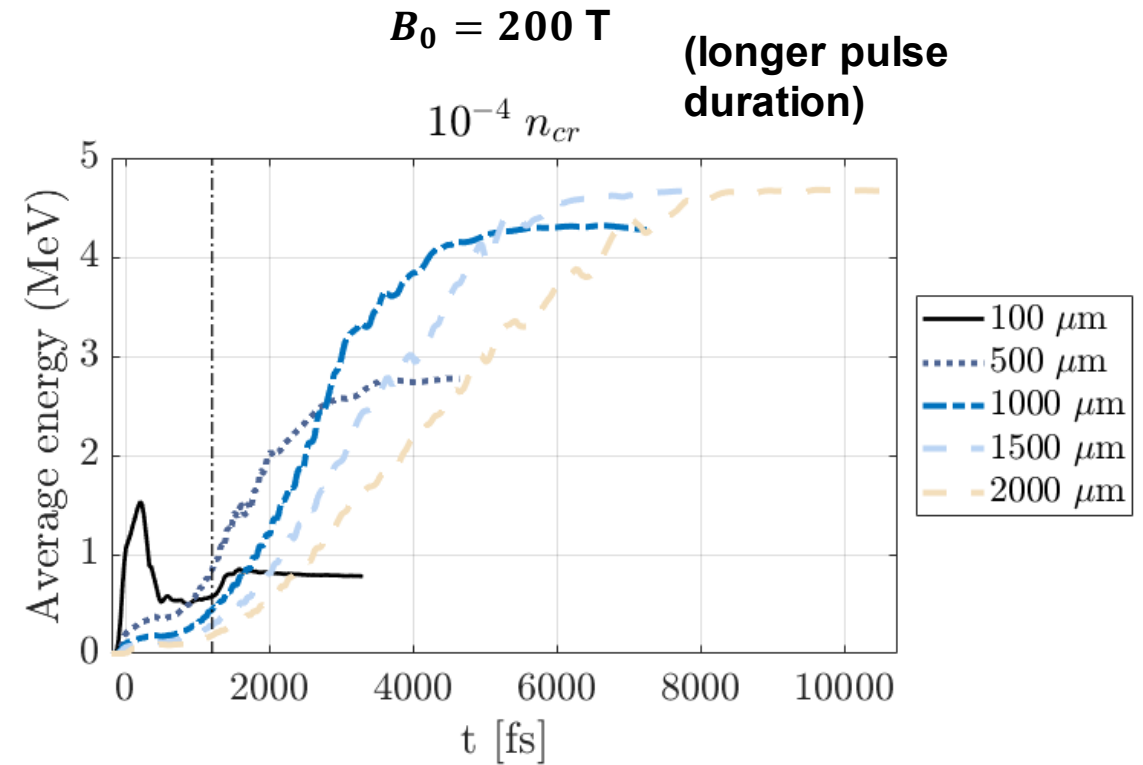
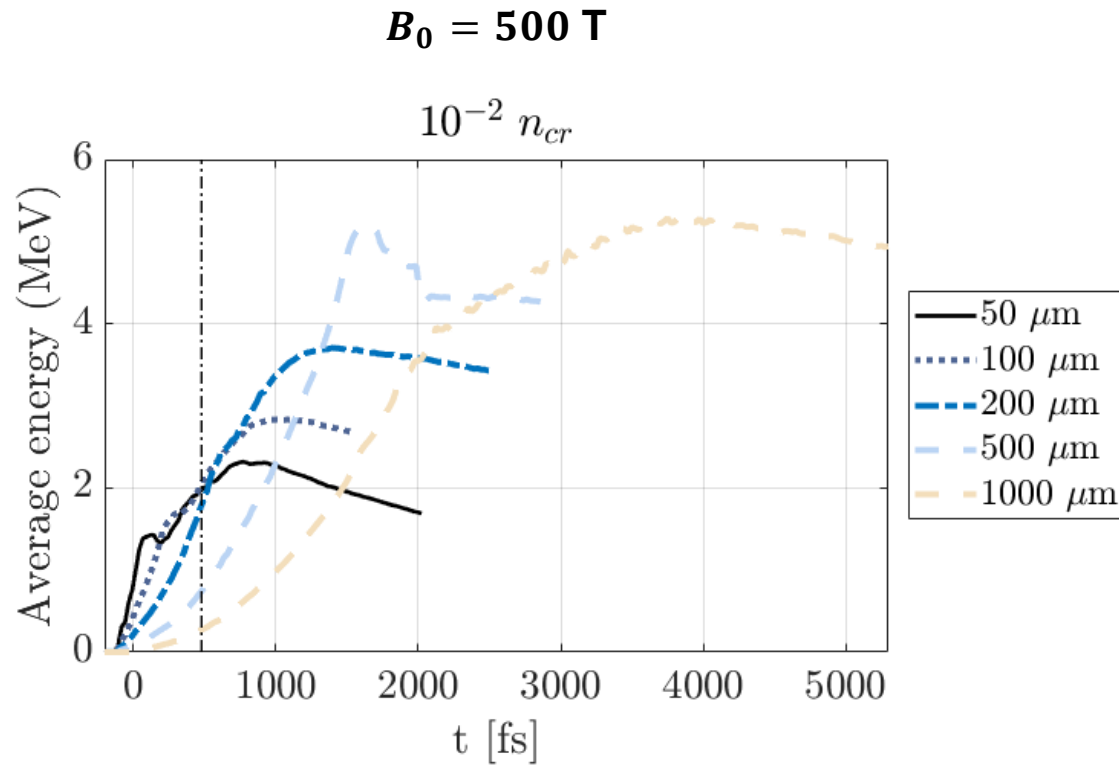
$$\frac{d\gamma}{ds} = \sqrt{1 - \frac{p_z^2}{p_y^2 + p_z^2}} \cdot \frac{\beta \sin \theta \frac{da}{ds}}{1 - \beta \cos \theta}$$

Heating is robust over $10^{-3} - 10^{-2} n_{cr}$, but breaks down for higher density



- Lasers substantially modify density profile for $10^{-3} n_{cr}$, but this does not appear to affect spectrum
- At lower density (e.g. $10^{-4} n_{cr}$), have $\omega_p < \omega_c$, which changes dynamics (based on 1D simulations)
- At higher density, charge separation E visibly interrupts cyclotron rotation

1D simulations predict even higher energy can be achieved in mm plasma, including with lower fields



Magnetically assisted DLA may be experimentally realizable using easily accessible plasma conditions